# The decrease of intraflagellar transport impairs sensory perception and metabolism in ageing

**Yincong Zhang**
CAS Center for Excellence in Molecular Cell Science, Shanghai Institute of Biochemistry and Cell Biology, Chinese Academy of Sciences

**Xiaona Zhang**
CAS Center for Excellence in Molecular Cell Science, Shanghai Institute of Biochemistry and Cell Biology, Chinese Academy of Sciences

**Yumin Dai**
CAS Center for Excellence in Molecular Cell Science, Shanghai Institute of Biochemistry and Cell Biology, Chinese Academy of Sciences

**Mengjiao Song**
Shanghai Institute of Biochemistry and Cell Biology, Chinese Academy of Sciences, University of Chinese Academy of Sciences

**Yifei Zhou**
Shanghai Institute of Biochemistry and Cell Biology, Chinese Academy of Sciences
https://orcid.org/0000-0003-0088-6262

**Jun Zhou**
Shandong Normal University https://orcid.org/0000-0003-3131-7804

**Xiumin Yan**
Shanghai Institutes for Biological Sciences, Chinese Academy of Sciences

**Yidong Shen** ( yidong.shen@sibcb.ac.cn )
CAS Center for Excellence in Molecular Cell Science, Shanghai Institute of Biochemistry and Cell Biology, Chinese Academy of Sciences https://orcid.org/0000-0002-2841-7233

---

**Article**

**Keywords:** ageing, declining sensory perception, impaired metabolism, intraflagellar transport, IFT, daf-19/RFX

**Posted Date:** July 30th, 2020

**DOI:** https://doi.org/10.21203/rs.3.rs-47370/v1

**Version of Record:** A version of this preprint was published at Nature Communications on March 19th, 2021. See the published version at https://doi.org/10.1038/s41467-021-22065-8.

# Abstract

Sensory perception and metabolic homeostasis deteriorate with ageing, impairing the health of aged animals. However, the mechanisms underlying their deterioration remain poorly understood. The potential interplay between the declining sensory perception and the impaired metabolism during ageing is also barely explored. Here, we report that the intraflagellar transport (IFT) in the cilia of sensory neurons is impaired in the aged nematode *Caenorhabditis elegans* due to a *daf-19*/RFX-modulated decrease of IFT components. The impaired IFT in sensory cilia in turn causes the deterioration of sensory perception with ageing. Moreover, whereas the IFT-dependent decrease of sensory perception in aged worms has a mild impact on the insulin/IGF-1 signalling, it remarkably suppresses AMP-activated protein kinase (AMPK) signalling across tissues. Upregulating *daf-19*/RFX effectively enhances IFT, sensory perception, AMPK activity and autophagy, promoting metabolic homeostasis and longevity. Our studies have uncovered an ageing pathway causing IFT decay and sensory perception deterioration, which in turn disrupts metabolism and healthy ageing.


# Introduction

Sensory perception is crucial to animal survival, not only for foraging and hazard avoidance but also for the regulation of metabolism[1]. Unfortunately, sensory perception declines with age, leading to one of the most common health problems in the aged population[2,3]. Despite its importance in health, the molecular mechanism of the ageing-induced deterioration of sensory perception remains poorly studied. The gradual loss of sensory neurons is considered as a major reason for the deteriorating sensory perception[4]. However, the nematode *Caenorhabditis elegans* (*C. elegans*), a well-established model organism for ageing research, exhibits olfactory deficits without losing any olfactory neurons[5,6]. In *C. elegans*, the neurocircuit of sensory perception starts from the cilia at the dendritic endings of sensory neurons, in a similar manner as olfactory perception in mammals[7–9]. A highly conserved intraflagellar transport (IFT) machinery, composed of motors and IFT complex proteins, delivers sensory receptors and other cargos bidirectionally along ciliary microtubules and is required for a functional cilium[10]. Despite the importance of sensory cilia in sensory perception, whether cilia degenerate with ageing and whether they cause the impairment of sensory perception in aged animals remain unexplored.

Metabolic homeostasis is critical in ageing. With ageing, the metabolic homeostasis is gradually disrupted, with catabolism (the breakdown of complex molecules to release energy) no longer matching with anabolism (the energy-consuming synthesis of complex molecules). Key catabolic pathways, such as autophagy, are dysregulated in aged animals[11,12]. Increasing catabolism or decreasing anabolism by modulating their pivotal regulators, TOR, AMP-activated protein kinase (AMPK) and insulin/IGF-1 signalling (IIS), was shown to effectively promote longevity by restoring metabolic homeostasis in various species[7]. Sensory perception is known to prime anabolism through activating pivotal anabolic pathways, such as IIS[1]. Consistently, mutating IFT genes extends the lifespan of the wild type (WT) worms through *daf-16*/FOXO, a critical transcription factor inhibited by IIS[13,14]. However, loss of sensory

perception also suppresses the longevity of the worms with mutated IGF receptor. Besides, olfactory dysfunction is shown to be an early predictor of mortality in old age[4,14]. Therefore, sensory perception may play a complex role in ageing. It is intriguing to explore whether improving sensory perception can induce longevity and whether other pathways in addition to IIS are involved in the sensory-ageing regulation. In aged animals, the impact of the impaired sensory perception on the disruption of metabolic homeostasis is also unclear.

Here, we report a critical cause of the ageing-induced deterioration of sensory perception in *C. elegans*. IFT in the sensory cilia is disrupted with ageing because of a *daf-19*/RFX-dependent dysregulation of IFT protein expression, and in turn impairs sensory perception. Moreover, our results indicate that sensory cilia activate AMPK signalling autonomously in sensory neurons by *par-4*/LKB1 and non-autonomously in other tissues through the neurotransmitter octopamine. The ageing-induced deterioration of sensory perception thus contributes to the disruption of metabolic homeostasis. Upregulating *daf-19*/RFX improves IFT, sensory perception, AMPK activity, and autophagy, promoting both health span and life span. These findings not only highlight the *daf-19*/RFX-IFT axis in the degeneration of cilia and sensory perception with ageing, but also underscore the sensory perception-induced AMPK signalling as a critical factor in the age-related disruption of metabolic homeostasis.

# Results

### The intraflagellar transport in sensory cilia deteriorates with ageing

To explore the effect of ageing on sensory perception, we first examined the response to food in young (day 1 of adulthood, D1) and aged worms (day 10 of adulthood, D10)[15]. Consistent with the age-related decline of chemotaxis[6,16], the food of bacteria no longer affected the movement of aged worms whereas young adults exhibited a clear enhanced slowing response (ESR) to bacteria (Fig. 1a and Supplementary Fig. 1a), indicating a defect of sensory perception with ageing. Cilia defects suppress dye-filling in sensory neurons[17]. Subsequent dye-filling assay indicated that the staining of DiI in the soma of sensory neurons became remarkably weaker at D10 (Fig. 1b), showing that ageing causes defects in the sensory cilia.

Despite the remarkable deterioration in cilia function, it has been shown that the microtubule organization in sensory cilia does not suffer any obvious changes in D10 worms[5], implying that the ciliary structure is unaffected by ageing at D10. We then examined IFT, which is crucial to cilia function, during ageing. The anterograde IFT is driven by kinesin and IFT-B complex, whereas the retrograde IFT by dynein and IFT-A complex (Fig. 1c). The motors of kinesin (OSM-3/KIF17), dynein (CHE-3/DHC2), and the core components of IFT-B (OSM-6/IFT52) and IFT-A (CHE-11/IFT140) complexes were endogenously GFP-tagged using genomic editing to visualize IFT *in vivo*. The length of GFP signal along cilia from CHE-3::GFP and CHE-11::GFP exhibited a slight increase in aged worms (Supplementary Fig. 1b and 1c). We next examined IFT using live imaging. Indeed, both the frequencies and velocities of these IFT components were remarkably decreased in the sensory cilia of aged worms (Fig. 1d to 1f, Supplementary Movie 1). As the rate of

ageing is highly variable among individuals[18], the decrease of IFT also exhibited a wide variation in aged worms (Supplementary Fig. 1d). *daf-2(-)* is a well-established longevity mutant with defective IIS [7]. Whereas IFT was impaired in D10 WT worms (Fig. 1), it was well-maintained in *daf-2(-)* mutants at D10 and D20 (Supplementary Fig. 2a to 2c, Supplementary Movie 2). Therefore, IFT is impaired with ageing but protected in the longevity mutant of *daf-2(-)*.

## DAF-19 is critical in the ageing-induced decline of IFT and sensory perception

The proper assembly of the multi-component IFT complexes is required for IFT. Inhibiting the expression of IFT complex components is known to suppress IFT[10,19]. Therefore, to explore the mechanism underlying the decreasing IFT with ageing, we examined the expression of IFT components in WT worms at D1 and D10. In the soma of amphid and phasmid sensory neurons, endogenously GFP-tagged OSM-3 and OSM-6, but not CHE-11 or CHE-3, exhibited a remarkable decrease with ageing in the WT worms. In phasmid sensory cilia, all four examined IFT components were reduced during ageing (Fig. 2a). DAF-19, an RFX transcription factor, is a master regulator of IFT genes in *C. elegans*[20]. Consistent with the decrease of IFT components with ageing, endogenously GFP-tagged DAF-19 was downregulated in the neurons of aged WT worms (Fig. 2b), implying that *daf-19* is critical in maintaining IFT during ageing. Indeed, a mild *daf-19* RNAi did not disrupt ciliogenesis but abolished the elevated motilities of OSM-3::GFP and OSM-6::GFP in *daf-2(-)* mutants at D10 to WT levels and substantially downregulated the velocity of CHE-3::GFP and CHE-11::GFP in *daf-2(-)* mutants (Supplementary Fig. 2d-2f). Mild overexpression of *daf-19c*, a *daf-19* isoform which specifically regulates ciliary genes, with its native promoter effectively ameliorated the decrease of DAF-19 in aged WT worms [20,21] (Fig. 2c). As a result, overexpressing *daf-19c* increased OSM-6::GFP, CHE-11::GFP, and CHE-3::GFP in young adult worms and upregulated all the examined IFT proteins in aged worms (Fig. 2d). The decrease of OSM-3::GFP and OSM-6::GFP with ageing was also suppressed by *daf-19c* overexpression (Fig. 2d). Following the increase of IFT proteins, both the velocity and frequency of the four examined IFT components were improved at D10 when *daf-19c* was upregulated. In young worms at D1, overexpressing *daf-19c* also increased the frequencies of CHE-3::GFP and CHE-11::GFP and the velocities of OSM-6::GFP and CHE-11::GFP (Fig. 3a to 3c, Supplementary Movie 3). Consistently, overexpressing *daf-19c* suppressed the diminishing DiI staining in sensory neurons with ageing (Fig. 3d). Therefore, a DAF-19-regulated decrease of IFT components underlies the age-related decline of IFT and in turn impairs the function of sensory cilia in aged worms.

We next performed chemotaxis assay to check whether the DAF-19-IFT-sensory cilia axis is also responsible for the deteriorating sensory perception with ageing. Because the worms at D10 suffer a severe decrease of motility and are not suitable for chemotaxis assay, worms at D5, which are at the end of their reproductive period, were examined. As expected, overexpressing *daf-19c* improved the chemotaxis to butanone at D5 (Fig. 3e, Supplementary Movie 4). Consistently, the response to food at D10 was also improved by upregulating *daf-19c* (Fig. 3f). Taken together, these results indicate that

overexpressing *daf-19c* effectively suppresses the ageing-induced degeneration of sensory cilia and perception.

## Food perception through sensory cilia activates AMPK signalling

Sensory perception, which requires proper IFT in sensory cilia, is tightly related to metabolism[1,10]. Since *daf-19*c controlled IFT underlies the age-related decline of sensory perception, we next examined its impact on metabolism. Metabolism is composed of the biosynthetic anabolism and the energy-yielding catabolism. In *C. elegans*, IFT is known to modulate insulin/IGF-1 signalling (IIS), a critical signalling pathway in anabolism[3,14]. IFT mutants of *osm-3(-)* and *osm-6(-)* exhibited severe cilia defects and IIS target genes were regulated as reported at D1[13,14] (Supplementary Fig. 3a). In aged worms, IIS exhibited a decreased modulation by sensory perception, as multiple IIS target genes were no longer changed upon mutating *osm-3* or *osm-6* at D10 (Supplementary Fig. 3a). Interestingly, overexpressing *daf-19c* failed to change IIS target genes expression in either young or aged worms (Supplementary Fig. 3b), implying that the enhanced sensory perception may not interfere with IIS.

We next examined the effect of sensory perception on AMPK, a pivotal driver of catabolism[22]. We first used western blot to check the level of activated AMPK (phosphorylated at the conserved Thr172, p-AMPK) in the whole worm. Overexpressing *daf-19c* in sensory neurons with its native promoter or in pan neurons with a neuron-specific promoter remarkably increased p-AMPK levels of both young and aged worms[20,21] (Fig. 4a and 4b). To examine whether this could be due to any side effects in larval development, we prepared another strain to overexpress *daf-19c::degron::gfp* by its native promoter. The overexpression of *daf-19c::degron::gfp* was suppressed by auxin treatment during larval stages and induced specifically in adulthood by removing auxin[23] (Supplementary Fig. 4a and 4b). Whereas inhibiting *daf-19c* upregulation in larvae effectively blocked the increase of p-AMPK in this strain at D1, the adulthood specific overexpression of *daf-19c* still enhanced p-AMPK level at D10 (Supplementary Fig. 4c). Therefore, it is unlikely that the *daf-19c*-induced p-AMPK is due to secondary effects in larval development. As western blot shows p-AMPK levels from the whole body, these results also imply that *daf-19c* could non-autonomously induce AMPK signalling in other tissues. Activated AMPK phosphorylates the CREB regulated transcriptional coactivator (CRTC-1) in *C. elegans* and induces its cytosolic translocation[24]. For further confirmation, we then examined the nuclear localization of CRTC-1::RFP in the intestine. As expected, overexpressing *daf-19c* reduced the nuclear localization of CRTC-1::RFP in the intestine (Fig. 4c), confirming that *daf-19c* in sensory neurons activates AMPK in other tissues.

To further test whether the *daf-19c*-induced AMPK activity is due to the enhanced sensory perception or other effects by *daf-19c* upregulation, worms were incubated in the plates with food, with food odour (food on the lid), or without food and examined for p-AMPK levels. The *daf-19c*-induced AMPK activation occurred only when worms sensed the food or food odour (Fig. 4a), indicating that it does require sensory perception, especially olfactory perception of food. Moreover, disrupting IFT and sensory cilia via mutating *osm-3* fully abolished the elevated p-AMPK levels in both young and aged worms

overexpressing *daf-19c* (Fig. 4d and Supplementary Fig. 4d). Therefore, *daf-19c* activates AMPK by enhancing IFT in sensory cilia and improving food perception. Consistently, when sensory cilia are disrupted by the mutation of *osm-3(-)* or *osm-6(-)*, p-AMPK levels decreased at D1 and D10 (Fig. 4d and Fig. 4e), confirming that sensory perception promotes AMPK activity. As *daf-19* controls innate immunity[25], worms were further incubated on UV-killed bacteria to minimize immunity response and examined for p-AMPK levels. *daf-19c* overexpression still robustly increased p-AMPK in worms fed with UV-killed bacteria (Supplementary Fig. 4f), indicating that this effect is independent of innate immunity.

Primary cilia in cultured cells modulate AMPK via LKB1, a kinase phosphorylating AMPK[26]. By tagging the worm ortholog of LKB1 (PAR-4) with GFP using genomic editing, we found that it was expressed in sensory neurons (Fig. 5a). RNAi against *par-4* specifically in sensory neurons or in all neurons blocked the increase of p-AMPK in worms overexpressing *daf-19c* (Fig. 5b and 5c), indicating that sensory cilia control AMPK activity via *par-4*. We further pursued the molecule transducing AMPK signalling non-autonomously from sensory neuron. Activated AMPK in neurons affects other tissues through octopamine[27]. To examine whether octopamine is required in the sensory perception-induced AMPK signalling, two octopamine biosynthetic enzymes (*tbh-1* and *tdc-1*) were mutated [27]. Indeed, mutating either of them blocked the increase of p-AMPK in worms overexpressing *daf-19c* (Fig. 5d and 5e). Supplementing the mutants of *tbh-1(-)* and *tdc-1(-)* with octopamine rescued the elevated p-AMPK induced by *daf-19c* overexpression (Fig. 5e). Therefore, octopamine is involved in the sensory perception-induced AMPK signalling.

## Sensory perception upregulates AMPK activity for metabolic homeostasis and longevity

Activated AMPK is a positive regulator of longevity, driving critical catabolic processes including autophagy[7]. Since enhanced sensory perception activates AMPK (Fig. 4 and 5), we next explored whether it also promotes autophagy in the intestine using a mCherry-GFP-tagged LGG-1 reporter. GFP in this reporter is specifically quenched in autolysosomes (ALs), thus labelling autophagosomes (APs) with both mCherry and GFP and ALs with mCherry[12]. As expected, upregulating *daf-19c* in sensory neurons remarkably increased the number of ALs whereas mildly reduced APs in the intestine (Fig. 6a). Either blocking or enhancing autophagy flux could change the numbers of APs and ALs. Chloroquine blocks autophagy flux and should not regulate APs and ALs when autophagy is already blocked[12]. Chloroquine suppressed the change of APs and ALs upon *daf-19c* overexpression (Fig. 6a), indicating that autophagy is active in the worms overexpressing *daf-19c* and enhanced sensory perception promotes autophagy in the intestine.

Metabolism is closely related to ageing. We next examined a series of hallmarks of healthy ageing in worms overexpressing *daf-19c*. Overexpressing *daf-19c* improved chemotaxis, the enhanced slowing response (ESR) to food, and motility in aged worms (Fig. 3e, 3f and 6b), which are key health metrics[15]. Interfering AMPK activity by neuron-specific RNAi against either *par-4*/LKB1 or *aak-2*/AMPK abrogated the enhanced motility in the worms overexpressing *daf-19c* at D10 (Supplementary Fig. 5a), indicating that sensory perception promotes healthy ageing through AMPK signalling. The motility of worms is

closely related to the integrity of myofibers in the body wall muscle (BWM), which is prone to ageing[18,28]. Sensory neuron specific overexpression of *daf-19c* reduced myofilaments abnormalities in aged worms, whereas a neuron-specific RNAi against *daf-19* had an adverse effect (Supplementary Fig. 5b and Supplementary Fig. 5c). AMPK and autophagy are critical in maintaining the balance of protein metabolism and in turn promote health and longevity[7]. The accumulation of polyglutamine (polyQ) aggregates is a marker of the deteriorating protein homeostasis[12]. Consistently, overexpressing *daf-19c* reduced polyQ aggregates (Fig. 6c), indicating improved protein homeostasis with the enhanced sensory perception. Taken together, sensory perception promotes healthy ageing through AMPK.

We next checked the potential effect of sensory perception on lifespan. With ageing, the motilities of IFT components decrease at variable rates among worms (Supplementary Fig. 1d). We then examined the lifespan of worms with remarkably different velocities of IFT components (i.e., OSM-3, OSM-6, and CHE-11) at D10. The worms with faster IFT lived longer than the worms with slower IFT (Fig. 6d and Supplementary Fig. 5d; Supplementary Table 3), showing a positive correlation between IFT function and longevity. We further examined the lifespan of the worms with improved sensory perception. Indeed, two strains overexpressing *daf-19c* with its native promoter, and another strain overexpressing *daf-19c* with a neuron-specific promoter all exhibited extended lifespans (Fig. 6e and Supplementary Fig. 5e; Supplementary Table 3). Disrupting sensory cilia by an adult-specific RNAi against *osm-3* abrogated the extended lifespan of the worms overexpressing *daf-19c* (Fig. 6f; Supplementary Table 3), indicating that *daf-19c* promotes longevity by enhancing sensory perception. Since sensory perception activates AMPK to improve worm motility (Supplementary Fig. 5a), neuron-specific RNAi against *par-4*/LKB1 or *aak-2*/AMPK was performed in adult worms to test whether the sensory perception-induced longevity also requires AMPK. Indeed, the lifespan of worms overexpressing *daf-19c* is reduced to the same level as the WT worms upon either of the two RNAi treatments (Fig. 6g; Supplementary Table 3). Therefore, sensory perception promotes longevity via upregulating AMPK signalling.

# Discussion

The decline of sensory perception is a hallmark of ageing[2]. However, its underlying mechanism remains poorly understood. Here, we report in the nematode *C. elegans* that the dysfunction of the sensory cilia, the start point of sensory circuit, is a major cause of the ageing-induced decrease of sensory perception. With ageing, a reduction of the master transcription factor of IFT genes, DAF-19/RFX, downregulates IFT components, disrupts the multiprotein IFT complexes, decreases IFT in the sensory cilium, and thereby impairs sensory perception. Upregulating *daf-19c* is an effective way to suppress these changes by rescuing the expression of IFT components in aged worms (Fig. 6h). Cilia are important regulators of cell survival and functions[29]. The dysfunction of cilia is known to impair neuronal activity[30,31]. Meanwhile, it is reported that brain injury induces cilia defects[31]. It will be interesting to pursue in future the intertwined interaction between cilia and neuronal activity. As the dysregulation of neurotransmitters and the loss of sensory neurons are involved in the age-related decrease of sensory perception, whether the degeneration of sensory cilia primes these changes is also an intriguing topic to explore[16,32,33].

Food perception without ingestion is known to drive insulin/IGF-1 signalling (IIS)[1]. Our results indicate that it also induces AMPK signalling and in turn autophagy. Therefore, food perception contributes to metabolic homeostasis before food intake by regulating the pivotal regulators of both anabolism (IIS) and catabolism (AMPK) (Fig. 6h). Interestingly, improving sensory perception upregulates AMPK activity but with little effect on IIS. This suggests different regulation thresholds of catabolism and anabolism by sensory perception and implies a metabolic protection against obesity when worms smell overabundant food. Consistently, increasing olfactory sensitivity suppresses diet-induced obesity in mice[34].

Metabolic homeostasis is disrupted by ageing[1]. Whereas the loss of sensory perception from birth extends lifespan by suppressing IIS[13,14], we show that the deterioration of sensory perception in aged worms disrupts the metabolic homeostasis by suppressing AMPK (Fig. 6h). Moreover, our results indicate that the regulation of sensory perception on IIS decreases while its control on AMPK signalling remains unchanged with ageing, suggesting that the modulation of sensory perception on metabolism shifts to AMPK in the aged worms. Consistently, autophagy, an essential catabolic progress under AMPK regulation, is also enhanced by improved sensory perception (Fig. 6h). Therefore, sensory perception improvement is an effective way to maintain metabolic homeostasis in aged worms by elevating catabolism, and in turn promotes healthy ageing and longevity. Consistently, disrupting sensory perception impairs lipid catabolism and WT worms with better sensory perception live longer[16,35] (Fig. 6). It has been a puzzle that disrupting sensory perception from birth increases the lifespan of WT worms by inhibiting IIS whereas suppresses the longevity of IIS-defective *daf-2(-)* mutants[13,14]. Our data suggest that this could be due to the decrease of AMPK activity when sensory perception is impaired. While the inhibited IIS causes an overwhelming longevity effect in the WT worms deprived of sensory perception from birth, blocking sensory perception in the IIS-defective *daf-2(-)* mutants has no more effect on IIS but inhibits the AMPK activity required for longevity and reduces the lifespan of *daf-2(-)* mutants. The ciliary function could also decline in aged people. Besides, loss of sensory perception is a risk factor to death and linked to many age-related diseases, such as obesity and neurodegenerative disease[1,4], suggesting that cilia could modulate ageing in human. As all the genes in this study are evolutionarily conserved, it will be interesting to see if similar pathways underlie age-related diseases and the metabolic changes in aged vertebrates.

# Materials And Methods

***C. elegans* strains and culture.** *C. elegans* strains used in this study are listed in Supplementary Table 1. *C. elegans* were grown on NGM plates with standard techniques at 20ºC[36]. All assayed worms were at day 1 of adulthood unless otherwise noted. Some strains were provided by CGC, which is funded by NIH Office of Research Infrastructure Programs (P40 OD010440). OP50 colonies on an NGM plate were treated with the sterilization program in a GS Gene Linker UV Chamber (BIO-RAD) for 15 m to obtain UV-killed bacteria. The killed bacteria were confirmed by no growth after O/N incubation in LB.

**Lifespan assays.** All lifespan assays were performed at 20ºC. For synchronization, L4 worms from eggs laid in a time window of 4 h or O/N were picked. Worms were transferred away from progeny to fresh plates every other day during the reproductive period. Worm survival was scored every two or three days. Worms undergoing internal hatching, bursting vulva, or crawling off the plates were censored. Worms not responding to prodding were scored as dead. Graphpad Prism (GraphPad Software) was used to plot survival curves and calculate median lifespan. Statistical analysis was performed with the Mantel-Cox Log Rank method.

For lifespan assays with correlated IFT velocities, individual N2 worms at day 10 of adulthood were anaesthetized using 5 mM levamisole and examined for IFT velocity on agar pads by live imaging microscopy. After imaging, worms were immediately recovered with M9 buffer and individually incubated in 35 mm NGM plates for ageing assay. At least 100 worms were tested in total.

**Plasmid construction.** All plasmids used in this study were constructed by Gibson Assembly. To generate *L3781-Pdaf-19c::daf-19c::mCherry*, 2,321 bp of the promoter and coding sequence of *daf-19c* were PCR amplified from N2 genomic DNA and cloned into *L3781-mCherry* [20]. To generate *L3781-Pdaf-19c::daf-19c::degron::gfp*, *degron::gfp* was amplified and insert into *L3781-Pdaf-19c::daf-19c. degron::gfp* was a gift from Ou Lab. To generate *L3781-Prab-3::daf-19c::mCherry*, *daf-19c* promoter was replaced by 1,357 bp of *rab-3* promoter in *Pdaf-19c::daf-19c::mCherry*. To generate *L3781-Pdyf-1::sid-1*, 454 bp of *dyf-1* promoter amplified from N2 genomic DNA and 2382 bp of *sid-1* cDNA amplified from N2 cDNA were cloned into *L3781* using Gibson Assembly[37].

For fluorescent tag knock-in, plasmids were constructed as described[38]. Briefly, sgRNAs for the target genes were selected from Zhang lab's CRISPR design tool at http://crispr.mit.edu and inserted into pDD162 (a gift from Bob Goldstein, Addgene #47549). Homology recombination templates were constructed by cloning the ~0.6 kb of 5' and 3' homology arms into pDD282 or pDD284 plasmids (gifts from Bob Goldstein, Addgene # 66823) using NEB Gibson Assembly kit. Target sites in the templates were modified with synonymous mutations. All tags were inserted at the C-terminal of genes of interest.

**Transgenes.** Extra-chromosomal transgenic lines of *daf-19c::mCherry* were obtained by co-injecting the plasmids of *L3781-Pdaf-19c::daf-19c::mCherry* and *Pmyo-3::CFP* or *Pegl-17::mCherry*, *L3781-Prab-3::daf-19c::mCherry* and *Pegl-17::mCherry* into N2. Plasmid concentrations for microinjections were 50 ng/ul for the genes of interest and 20 ng/ul for injection marker, respectively.

For knock-in lines, injections and subsequent screens were performed as described[38]. Self-excising selection cassettes were discarded before sequencing and phenotypic analysis. The *par-4(syb1018)V* allele was generated by SunyBiotech using CRISPR/Cas9 technology. mNeonGreen-3xFLAG were inserted into the C-terminal of the endogenous *par-4* gene. All knock-in strains were verified by DNA sequencing.

**RNA interference.** RNAi experiments were performed using *E.coli* HT115 bacteria on standard NGM plates containing 100 mg/ml ampicillin and 0.8 mM IPTG as described[39]. Worms were grown on HT115

expressing dsRNA against indicated genes from the egg until the corresponding time unless otherwise noted. HT115 expressing dsRNA against *luc2*, a real but not worm gene, served as a control to minimize off-target phenotypes. The strain of HT115 [*L4440::luc2*] was a gift from Antebi lab (MPI-AGE). For neuron-specific RNAi, TU3401 worms were used directly or after crossed with indicated strains. For sensory neuron specific RNAi, SYD0779 (*sid-1(pk3321) V; sydEx196[pdyf-1::sid-1, egl-17p::mCherry]*) were used directly or after crossed with indicated strains.

**Quantitative RT-PCR.** More than 100 well-fed synchronized worms were collected into QIAzol reagent (QIAGEN), and column purified by RNeasy Mini (QIAGEN). cDNA was subsequently generated by iScriptTM Reverse Transcription Supermix for RT-qPCR (Bio-Rad). Quantitative RT-PCR was performed with Bestar® Sybr Green qPCR Master Mix (DBI Bioscience) or 2xNovoStart® SYBR qPCR SuperMix Plus (Novoprotein) on a QuantStudioTM 6 Flex Real-time PCR System (Applied Biosystems) or a CFX384 TouchTM Real-Time PCR Detection System (Bio-Rad). mRNA levels of *ama-1* and *cdc-42* were used for normalization. Four technical replicates were performed in each reaction. At least three biological repeats were taken. Primer sequences are listed in Supplementary Table 2.

**Microscopy.** Live imaging of intraflagellar transport was performed following a previous report[40]. In brief, worms were anaesthetized with 5 mM levamisole in M9 buffer, mounted on 5% agar pads, and maintained at room temperature. Images were collected using an Olympus IX81 microscope equipped with a 100x, 1.49 NA objective and an Ultraview spinning disc confocal head (PerkinElmer Ultra VIEW VoX). Time-lapse images were acquired at an exposure time of 200 ms for 30 s (spinning disk). Cilia were chosen based on their orientation plane, with the base, proximal segment, and distal segment in focus.

Fluorescence images were obtained using a Leica TCS SP8 confocal microscope or an Olympus BX53 microscope. Animals were anaesthetized using 5 mM levamisole and mounted on 5% agar pads. Fluorescent intensities were measured by ImageJ[41].

For the analysis of abnormalities in body wall muscle, MYO-3::GFP in the body wall muscle was imaged. The abnormalities were characterized into two types: a general disorganization of the myofilaments with GFP aggregations and gaps in the lattice[28].

For the analysis of polyQ strains, the numbers of polyQ aggregates in the body wall muscle were counted in individual worms at day 3 of adulthood. For each genotype, at least 56 animals from three independent experiments were scored.

**Kymograph generation and analysis.** Kymographs were generated and analyzed as described [40]. In brief, Fourier filtered and separated anterograde or retrograde kymographs were generated with the KymographClear toolset plugin in ImageJ (http://www.nat.vu.nl/~erwinp/downloads.html). IFT velocities at every 0.5 mm along cilia were measured by the KymographDirect software (http://www.nat.vu.nl/~erwinp/downloades.html) from the kymographs. Velocity curves were

subsequently generated using GraphPad Prism (GraphPad Software). Cilia with projection lengths smaller than 7 mm were not examined.

**Autophagy analysis.** mCherry::GFP::LGG-1 puncta in posterior intestinal cells were counted from about 5 slices with 1 μm step size, the Z-position was selected where intestinal nucleus could be seen clearly. The puncta were counted using ComDet v.0.3.7 in ImageJ. For each genotype, at least 20 worms at corresponding stages from three independent experiments were scored. The number of APs was calculated by the GFP-positive puncta, and the number of ALs was calculated by the puncta with only mCherry signal.

**Western blotting.** Synchronized worms were grown to indicated ages and harvested in M9. To test the effect of food perception on *daf-19c*-induced p-AMPK, worms at day 1 of adulthood were washed off plates and further washed three times by M9 buffer before transferred to prepared 90-mm plates for the test. Three groups of plates were set up: a. plates seeded with OP50 (food and odour); b. empty plates with OP50 only on lids (odour); c. empty plates (no food or odour). After 1 or 12 h, worms were collected in M9 for western blotting to test p-AMPK level.

After three rounds of washing with M9, 4x SDS gel-loading buffer (Takara, Cat#9173) was added into worm samples and kept at -80°C. Proteins were separated by reducing SDS-PAGE and transferred to PVDF membranes. Membranes were then blotted with antibodies against p-AMPK (CST, Cat# 4188s, dilution: 1:1,000) and a-tubulin (Sigma-Aldrich, Cat# T5168, dilution: 1:2,000). An anti-mouse secondary antibody conjugated with horseradish peroxidase (Life Technologies, Cat# G21040, 1:5,000) was used for detecting anti-a-tubulin, and an anti-rabbit secondary antibody (Life Technologies, Cat# G21234, 1:5,000) was used for detecting anti-p-AMPK primary antibodies. Signals of western blotting were measured using Adobe Photoshop. Background signals were subtracted as reported[42].

**Dye-filling assay.** DiI staining was performed as described with modifications[43]. Approximately 20-30 day 1 or day 10 adult worms were randomly picked into 200 ml M9 solution. After washing with M9 for three times to remove bacterial, worms were incubated with 1 mg/ml fluorescent Dye (DiI 1,1'-dioctadecyl-3,3,30,30,-tetramethylindo-carbocyanine perchlorate, Sigma) in dark at room temperature for 30 min. Worms were subsequently washed with M9 and transferred to regular NGM plates for 30 min. For imaging by an Olympus BX53 microscope, worms were mounted on 5% agarose pads and anaesthetized with 5 mM levamisole. At least three independent assays were performed.

**Auxin treatment**. Auxin treatment was performed by transferring worms to bacteria-seeded plates containing auxin as reported[23]. The natural auxin indole-3-acetic acid (IAA) (Alfa Aesar, #A10556) was prepared as a 400 mM stock solution in ethanol. Auxin was diluted into the NGM agar at 1 mM.

**Enhanced slowing response assay.** Enhanced slowing responses (ESR) were performed as described with modification[44]. About 20 food-deprived worms were washed free of bacterial in M9 buffer and then transferred to NGM plates that had no bacterial or a ring-like bacterial lawn in the middle. The worms

were incubated on these plates for 30 min at room temperature before their body bends was recorded. For the worms on the plate with bacteria, only those on the bacteria lawn were scored.

**Chemotaxis assay.** Chemotaxis assay was performed as described with modification[45]. In brief, on a 6-cm unseeded plate, 1 ml of 1M $NaN_3$ were spotted at the odourant spot with 1 ml of 10% butanone and the control spot with 1 ml of 95% ethanol freshly before assay. Around 200 synchronized worms at indicated ages were placed at the centre of the plate (origin) and recorded by a Nikon D4 camera for their movement for 1 h. Chemotaxis index (CI) was calculated at the end of the assay as: $CI=(N_{butanone}-N_{ethanol})/(N_{total}-N_{origin})$. The worms were counted by the ComDet plugin in ImageJ (https://github.com/ekatrukha/ComDet/wiki).

**Motility assay.** Worms were transferred into a M9-filled 96-well plate with one in each well recorded using an Olympus SZX16 stereomicroscope equipped with a Nikon D4 camera. The thrashing rate was subsequently scored from videos. For each genotype or treatment, around 20 animals were examined in each of the three replicates.

**Statistical analysis.** Results are presented as Mean±SD unless otherwise noted. Statistical tests were performed as indicated using GraphPad Prism (GraphPad Software). Detailed statistical information is shown in Supplementary Table 3.

# Declarations


### Acknowledgements

We thank Dr. Jindong Han (Peking U.) for plasmids, Dr. Adam Antebi (MPI-AGE) and CGC for strains, Drs. Guangshuo Ou (Tsinghua U.) and Yixian Zheng (Carnegie Institution for Science) for helpful discussion and Mr. Chenghui Wan for illustration. This research was supported by the Thousand Talents Plan (Youth), the Strategic Priority Research Program of the Chinese Academy of Sciences, Grant No. XDB19000000, and NSFC, Grant No. 91749119.


### Author contributions

Y.Z., X.Z., X.Y., and Y.S. conceived the project and designed the experiments. Y.Z. and X.Z. performed experiments and analyzed data, with the assistance of Y.D. and M.S.. Y.Z. performed autophagy assays. J.Z. helped in live imaging microscopy. Y.Z., X.Y., and Y.S. wrote the manuscript. All authors contributed to manuscript editing.

### Competing interests

Authors declare no competing interests.


**Correspondence and requests for materials** should be addressed to and will be fulfilled by Yidong Shen (yidong.shen@sibcb.ac.cn).

# References


1. Riera, C. E. & Dillin, A. Emerging Role of Sensory Perception in Aging and Metabolism. *Trends in endocrinology and metabolism: TEM* 27, 294–303, doi:10.1016/j.tem.2016.03.007 (2016).
2. 10.1093/geronb/gbp048
   Schumm, L. P. *et al.* Assessment of sensory function in the National Social Life, Health, and Aging Project. *The journals of gerontology. Series B, Psychological sciences and social sciences* 64 Suppl 1, i76-85, doi:10.1093/geronb/gbp048 (2009).
3. Linford, N. J., Kuo, T. H., Chan, T. P. & Pletcher, S. D. Sensory perception and aging in model systems: from the outside in. *Annual review of cell and developmental biology* 27, 759–785, doi:10.1146/annurev-cellbio-092910-154240 (2011).
4. Doty, R. L. & Kamath, V. The influences of age on olfaction: a review. *Frontiers in psychology* 5, 20, doi:10.3389/fpsyg.2014.00020 (2014).
5. Herndon, L. A., Wolkow, C. A., Driscoll, M. & Hall, D. H. in *Ageing: Lessons from C. elegans* (eds Anders Olsen & Matthew S. Gill) 9–39 (Springer International Publishing, 2017).
6. Cai, S. Q. & Sesti, F. Oxidation of a potassium channel causes progressive sensory function loss during aging. *Nature neuroscience* 12, 611–617, doi:10.1038/nn.2291 (2009).
7. Kenyon, C. J. The genetics of ageing. *Nature* 464, 504–512, doi:10.1038/nature08980 (2010).
8. Inglis, P. N., Ou, G., Leroux, M. R. & Scholey, J. M. The sensory cilia of Caenorhabditis elegans. *WormBook: the online review of C. elegans biology*, 1–22, doi:10.1895/wormbook.1.126.2 (2007).
9. Falk, N., Losl, M., Schroder, N. & Giessl, A. Specialized Cilia in Mammalian Sensory Systems. *Cells* 4, 500–519, doi:10.3390/cells4030500 (2015).
10. Lechtreck, K. F. IFT-Cargo Interactions and Protein Transport in Cilia. *Trends in biochemical sciences* 40, 765–778, doi:10.1016/j.tibs.2015.09.003 (2015).
11. Chang, J. T. & Hansen, M. Age-associated and tissue-specific decline in autophagic activity in the nematode C. elegans. *Autophagy* 14, 1276–1277, doi:10.1080/15548627.2018.1445914 (2018).
12. Zhou, Y. *et al.* A secreted microRNA disrupts autophagy in distinct tissues of Caenorhabditis elegans upon ageing. *Nature communications* 10, 4827, doi:10.1038/s41467-019-12821-2 (2019).
13. Alcedo, J. & Kenyon, C. Regulation of C. elegans longevity by specific gustatory and olfactory neurons. *Neuron* 41, 45–55 (2004).
14. Apfeld, J. & Kenyon, C. Regulation of lifespan by sensory perception in Caenorhabditis elegans. *Nature* 402, 804–809, doi:10.1038/45544 (1999).
15. Sawin, E. R., Ranganathan, R. & Horvitz, H. R. C. elegans locomotory rate is modulated by the environment through a dopaminergic pathway and by experience through a serotonergic pathway. *Neuron* 26, 619–631 (2000).
16. Leinwand, S. G. *et al.* Circuit mechanisms encoding odors and driving aging-associated behavioral declines in Caenorhabditis elegans. *eLife* 4, e10181, doi:10.7554/eLife.10181 (2015).

17. Herman, R. K. Analysis of Genetic Mosaics of the Nematode Caenorhabditis-Elegans. *Genetics* 108, 165–180 (1984).
18. Herndon, L. A. *et al.* Stochastic and genetic factors influence tissue-specific decline in ageing C. elegans. *Nature* 419, 808–814, doi:10.1038/nature01135 (2002).
19. Mohamed, M. A. A., Stepp, W. L. & Okten, Z. Reconstitution reveals motor activation for intraflagellar transport. *Nature*, doi:10.1038/s41586-018-0105-3 (2018).
20. Senti, G. & Swoboda, P. Distinct isoforms of the RFX transcription factor DAF-19 regulate ciliogenesis and maintenance of synaptic activity. *Molecular biology of the cell* 19, 5517–5528, doi:10.1091/mbc.E08-04-0416 (2008).
21. Burghoorn, J. *et al.* The in vivo dissection of direct RFX-target gene promoters in C. elegans reveals a novel cis-regulatory element, the C-box. *Developmental biology* 368, 415–426, doi:10.1016/j.ydbio.2012.05.033 (2012).
22. Herzig, S. & Shaw, R. J. AMPK: guardian of metabolism and mitochondrial homeostasis. *Nature reviews. Molecular cell biology* 19, 121–135, doi:10.1038/nrm.2017.95 (2018).
23. Zhang, L., Ward, J. D., Cheng, Z. & Dernburg, A. F. The auxin-inducible degradation (AID) system enables versatile conditional protein depletion in C. elegans. *Development* 142, 4374–4384, doi:10.1242/dev.129635 (2015).
24. Mair, W. *et al.* Lifespan extension induced by AMPK and calcineurin is mediated by CRTC-1 and CREB. *Nature* 470, 404–408, doi:10.1038/nature09706 (2011).
25. Xie, Y., Moussaif, M., Choi, S., Xu, L. & Sze, J. Y. RFX transcription factor DAF-19 regulates 5-HT and innate immune responses to pathogenic bacteria in Caenorhabditis elegans. *PLoS genetics* 9, e1003324, doi:10.1371/journal.pgen.1003324 (2013).
26. Boehlke, C. *et al.* Primary cilia regulate mTORC1 activity and cell size through Lkb1. *Nature cell biology* 12, 1115–1122, doi:10.1038/ncb2117 (2010).
27. Burkewitz, K. *et al.* Neuronal CRTC-1 governs systemic mitochondrial metabolism and lifespan via a catecholamine signal. *Cell* 160, 842–855, doi:10.1016/j.cell.2015.02.004 (2015).
28. Meissner, B. *et al.* An integrated strategy to study muscle development and myofilament structure in Caenorhabditis elegans. *PLoS genetics* 5, e1000537, doi:10.1371/journal.pgen.1000537 (2009).
29. Wheway, G., Nazlamova, L. & Hancock, J. T. Signaling through the Primary Cilium. *Frontiers in cell and developmental biology* 6, 8, doi:10.3389/fcell.2018.00008 (2018).
30. Lee, J. E. & Gleeson, J. G. Cilia in the nervous system: linking cilia function and neurodevelopmental disorders. *Current opinion in neurology* 24, 98–105, doi:10.1097/WCO.0b013e3283444d05 (2011).
31. Kirschen, G. W. & Xiong, Q. Primary cilia as a novel horizon between neuron and environment. *Neural regeneration research* 12, 1225–1230, doi:10.4103/1673-5374.213535 (2017).
32. Attems, J., Walker, L. & Jellinger, K. A. Olfaction and Aging: A Mini-Review. *Gerontology* 61, 485–490, doi:10.1159/000381619 (2015).

33. Bressler, N. M. Age-related macular degeneration is the leading cause of blindness. *Jama* 291, 1900–1901, doi:10.1001/jama.291.15.1900 (2004).
34. Xu, J. *et al.* The voltage-gated potassium channel Kv1.3 regulates energy homeostasis and body weight. *Human molecular genetics* 12, 551–559, doi:10.1093/hmg/ddg049 (2003).
35. Mutlu, A. S., Gao, S. M., Zhang, H. & Wang, M. C. Olfactory specificity regulates lipid metabolism through neuroendocrine signaling in Caenorhabditis elegans. *Nature communications* 11, 1450, doi:10.1038/s41467-020-15296-8 (2020).
36. Brenner, S. The genetics of Caenorhabditis elegans. *Genetics* 77, 71–94 (1974).
37. Boehm, M. & Slack, F. A developmental timing microRNA and its target regulate life span in C. elegans. *Science* 310, 1954–1957, doi:10.1126/science.1115596 (2005).
38. Dickinson, D. J., Pani, A. M., Heppert, J. K., Higgins, C. D. & Goldstein, B. Streamlined Genome Engineering with a Self-Excising Drug Selection Cassette. *Genetics* 200, 1035–1049, doi:10.1534/genetics.115.178335 (2015).
39. Kamath, R. S., Martinez-Campos, M., Zipperlen, P., Fraser, A. G. & Ahringer, J. Effectiveness of specific RNA-mediated interference through ingested double-stranded RNA in Caenorhabditis elegans. *Genome biology* 2, RESEARCH0002, doi:10.1186/gb-2000-2-1-research0002 (2001).
40. Prevo, B., Mangeol, P., Oswald, F., Scholey, J. M. & Peterman, E. J. Functional differentiation of cooperating kinesin-2 motors orchestrates cargo import and transport in C. elegans cilia. *Nat Cell Biol* 17, 1536–1545, doi:10.1038/ncb3263 (2015).
41. Hartig, S. M. Basic image analysis and manipulation in ImageJ. *Curr Protoc Mol Biol Chap. 14*, Unit14 15, doi:10.1002/0471142727.mb1415s102 (2013).
42. King, J. M., Hays, T. S. & Nicklas, R. B. Dynein is a transient kinetochore component whose binding is regulated by microtubule attachment, not tension. *Journal of Cell Biology* 151, 739–748, doi:DOI 10.1083/jcb.151.4.739 (2000).
43. 10.1016/j.cub.2017.04.015
Yi, P., Li, W. J., Dong, M. Q. & Ou, G. Dynein-Driven Retrograde Intraflagellar Transport Is Triphasic in C. elegans Sensory Cilia. *Curr Biol* 27, 1448–1461 e1447, doi:10.1016/j.cub.2017.04.015 (2017).
44. Sawin, E. R., Ranganathan, R. & Horvitz, H. R. C-elegans locomotory rate is modulated by the environment through a dopaminergic pathway and by experience through a serotonergic pathway. *Neuron* 26, 619–631, doi:Doi 10.1016/S0896-6273(00)81199-X (2000).
45. Kauffman, A. *et al.* C. elegans positive butanone learning, short-term, and long-term associative memory assays. *Journal of visualized experiments: JoVE*, doi:10.3791/2490 (2011).

# Supplementary Movies

Supplementary movies were not provided with this version.

# Figures

## Fig. 1 Zhang et.al

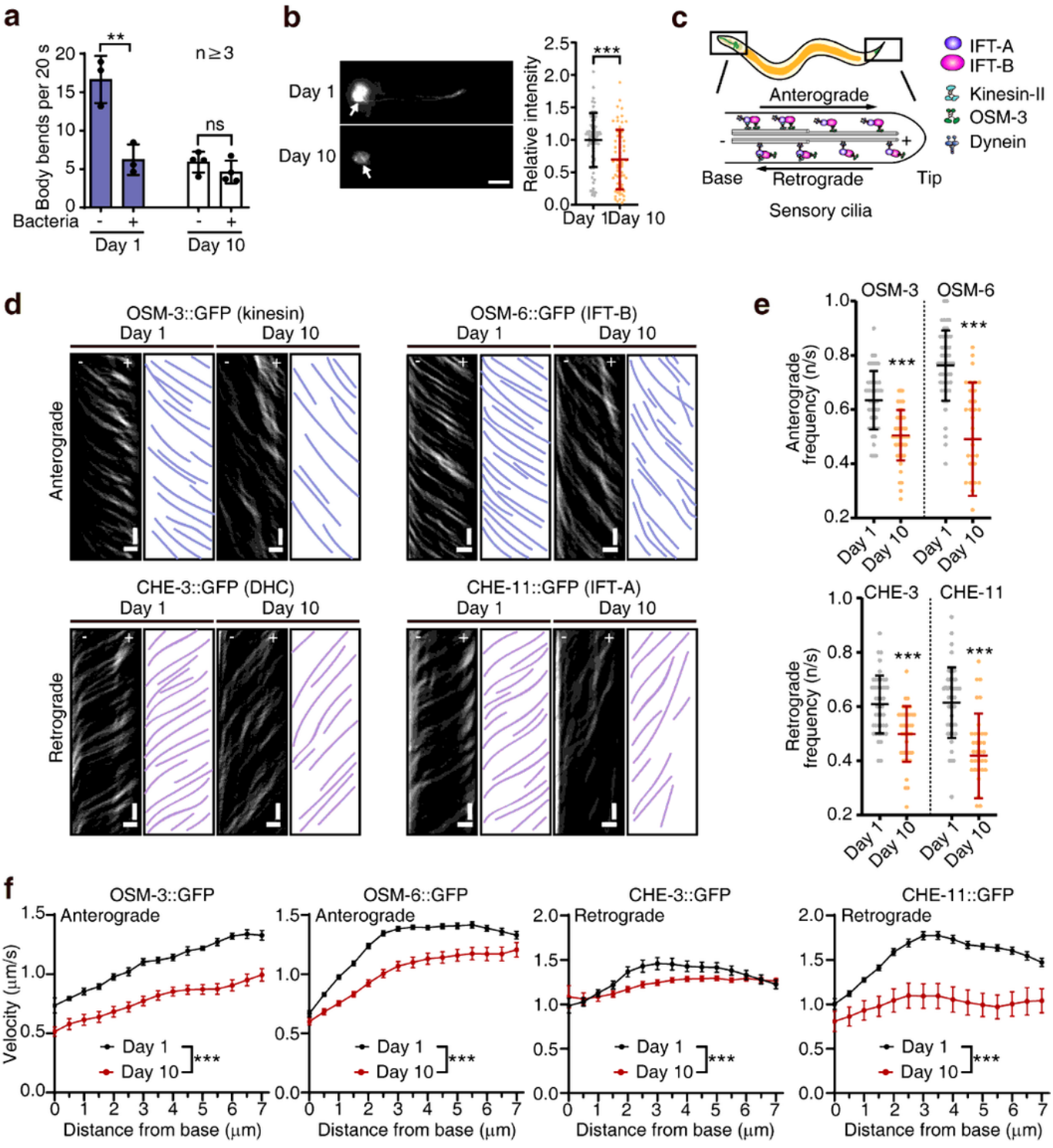


### Figure 1

The intraflagellar transport (IFT) in the sensory cilia is impaired by ageing. a. The enhanced slowing response to the food of worms at indicated ages. Sensing the food reduces worm movement (body bends). The worms at day 10 of adulthood are over the reproductive age and exhibit ageing features. b. The DiI staining is decreased in the sensory neurons of aged worms. Arrows denote the soma of sensory neurons. Scale bar: 10 μm. c. A depiction of IFT in sensory cilia, which are at the dendritic endings of

sensory neurons. IFT-B complex and kinesin control the anterograde IFT, whereas IFT-A complex and dynein modulate the retrograde IFT. d-f. IFT decreases with ageing. Representative IFT components were examined at indicated ages. The representative kymographs (d), frequencies (e), and velocities (f) are respectively shown. (+) and (-) denote microtubule polarity. Horizontal scale bars: 2 μm; vertical scale bars: 2 s. Error bars in IFT velocities are SEM, the rest are SD. Two-way ANOVA in (f), and Unpaired t-test in the rest, ** p<0.01, *** p<0.001, ns: non-significant.

**Fig. 2 Zhang et.al**

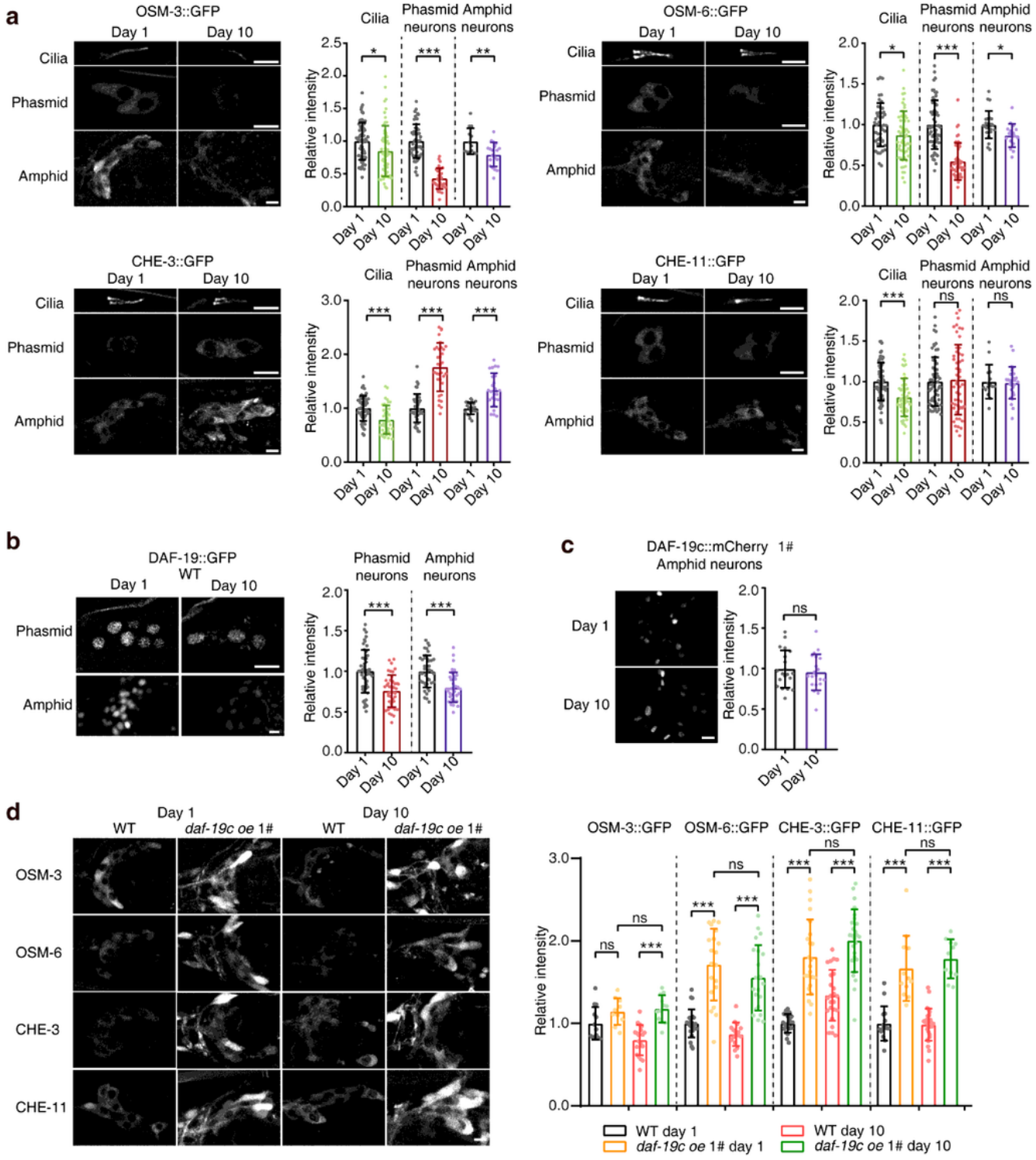


**Figure 2**

IFT components are downregulated with ageing in a DAF-19/RFX dependent manner. a. The expression of the indicated IFT components in the phasmid cilia and the soma of phasmid and amphid neurons of WT worms at indicated ages. The tested proteins were endogenously tagged with GFP using CRISPR/Cas9 technology. Scale bars: 5 μm. b. The expression of endogenously tagged DAF-19::GFP in the soma of phasmid and amphid neurons of WT worms at indicated ages. Scale bars: 5 μm. c. The expression of DAF-19c::mCherry in the soma of amphid neurons at indicated ages. Scale bar: 5 μm. d. The expression of IFT components in the amphid neuron soma in the indicated strains at day 1 and day 10 of adulthood. The worms overexpressing daf-19c were examined in parallel to the WT worms in A. Scale bar: 5 μm. Error bars are SD. Unpaired t-test, * $p<0.05$, ** $p<0.01$, *** $p<0.001$, ns: non-significant.

**Fig. 3 Zhang et.al**

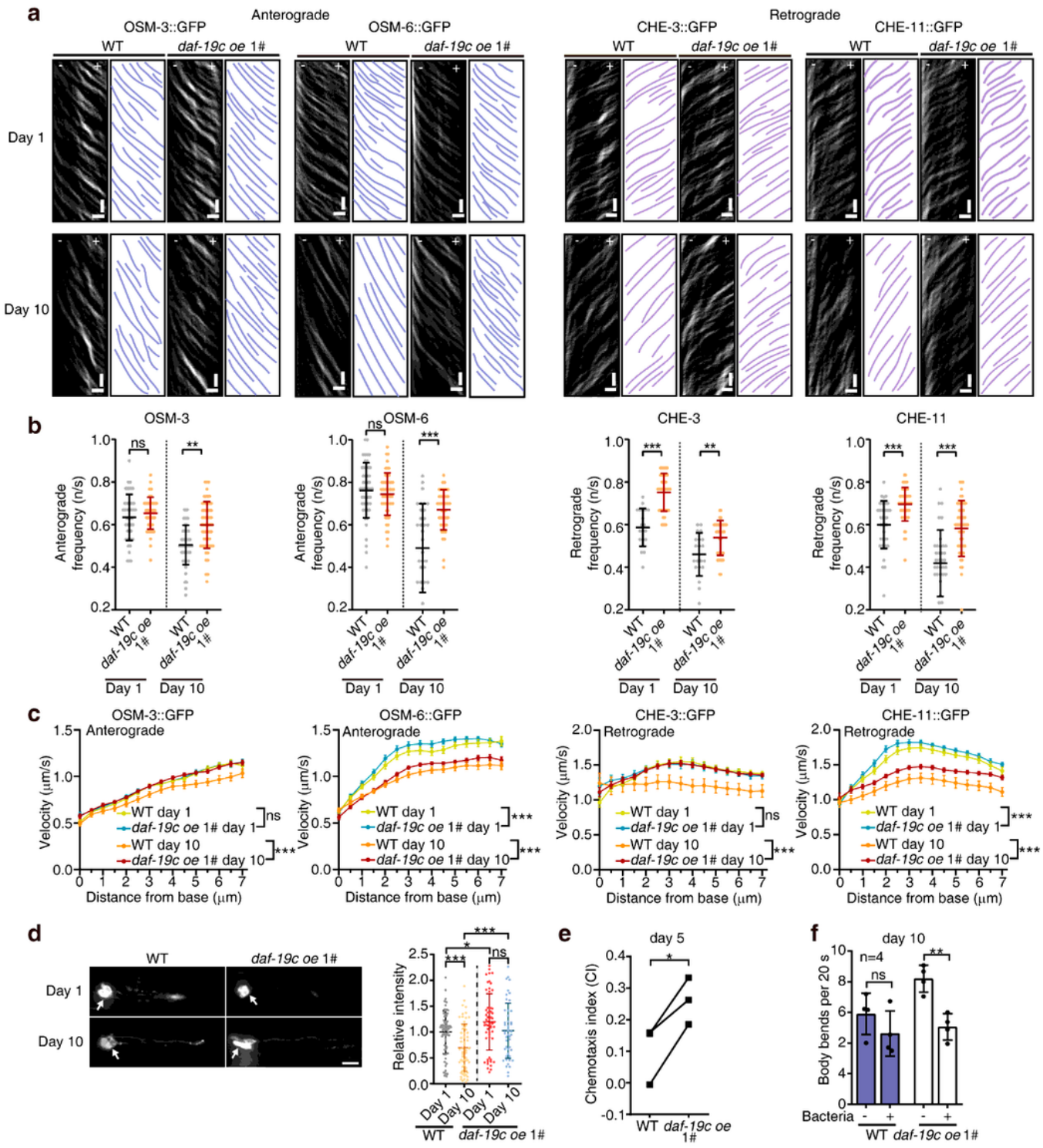


## Figure 3

Overexpressing daf-19/RFX enhances IFT and sensory perception in the aged worms. a-c. Overexpressing daf-19c with its native promoter increases IFT in the sensory cilia at indicated ages. Representative kymographs, frequencies, and velocities are respectively shown in (a), (b), and (c). Horizontal scale bars: 2 μm; vertical scale bars: 2 s. d. Overexpressing daf-19c rescues the impaired DiI staining in the aged sensory neurons. Arrows denote the soma. The assay was performed in parallel with Fig. 1b. Scale bar:

10 μm. e. Chemotaxis assay of indicated strains at day 5 of adulthood. f. daf-19c overexpression improves the response to food in the aged worms. Note that a decrease in body bends upon feeding indicates the response to food. Error bars in IFT velocities are SEM, the rest are SD. Two-way ANOVA in (c), paired t-test in (e), unpaired t-test in the rest, * p<0.05, ** p<0.01, *** p<0.001, ns: non-significant.

**Fig. 4 Zhang et.al**

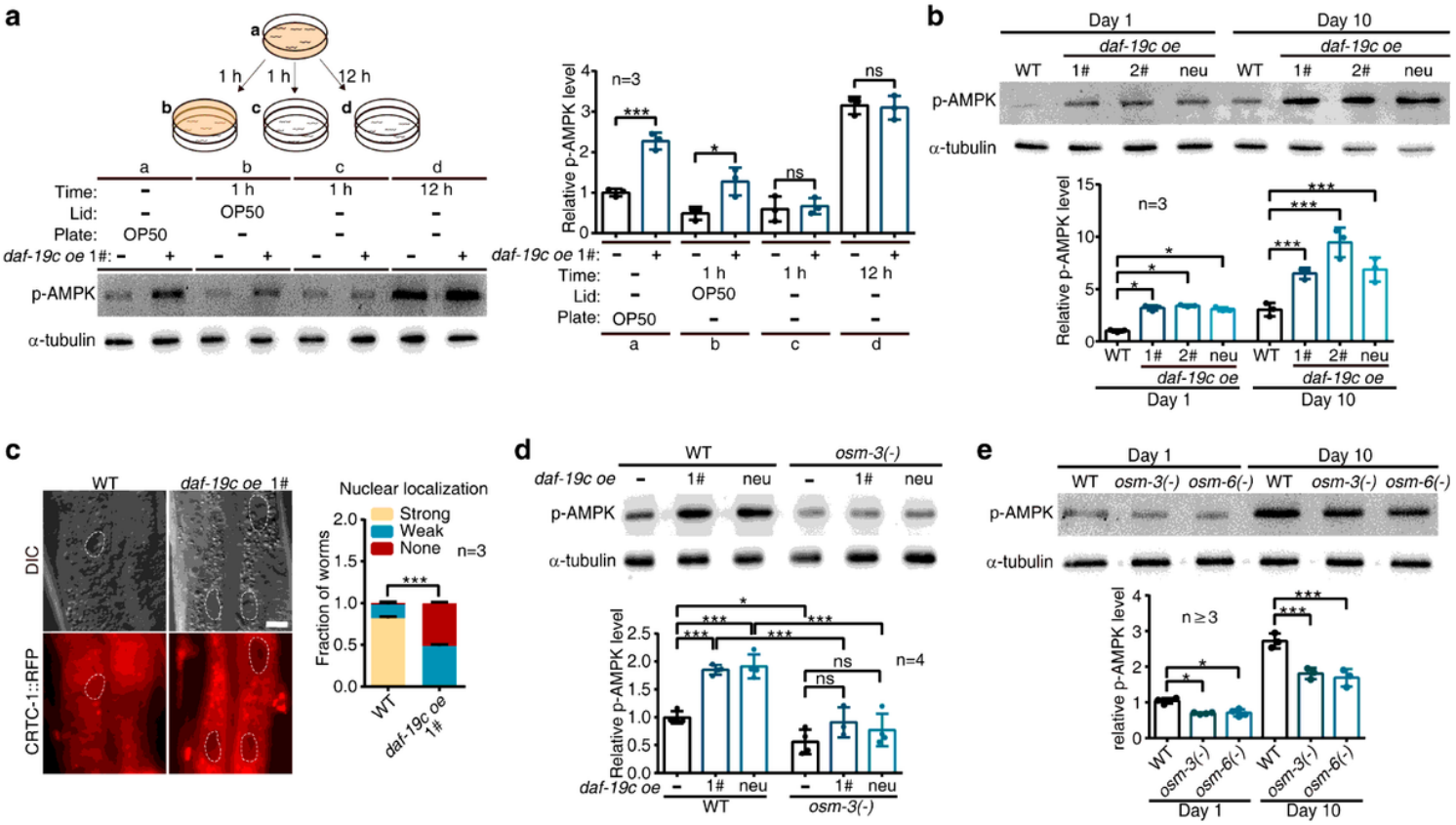


## Figure 4

The sensory cilia induce AMPK activity across tissues. a. The phosphorylation levels of AMPK (p-AMPK) in young WT worms subjected to indicated treatments. The bacteria of OP50 (orange) is the food of C. elegans. Note that daf-19 upregulates p-AMPK only when worms are fed (OP50 in the plate, a) or smell the food (OP50 on the lid, b). b. Overexpressing daf-19c by its native promoter (1# and 2#) or a neuron-specific promoter (neu) increases p-AMPK levels in both young and aged worms. c. Overexpressing daf-19c reduces the nuclear localization of CRTC-1::RFP in the intestinal cells. Dotted lines denote the nucleus of intestinal cells. Scale bar: 25 μm. d. Disrupting cilia by mutating osm-3 suppresses the increase of p-AMPK in the worms overexpressing daf-19c at day 1 of adulthood by its native promoter (1#) or a neuron-specific promoter (neu). e. p-AMPK levels decrease in worm mutants with defected cilia (osm-3(-), osm-6(-)). α-tubulin serves as loading controls in western blot assays. Error bars: SD. Two-way ANOVA in (c), and one-way ANOVA in the rest. * p<0.05, *** p<0.001, ns: non-significant.

**Fig. 5 Zhang et al.**

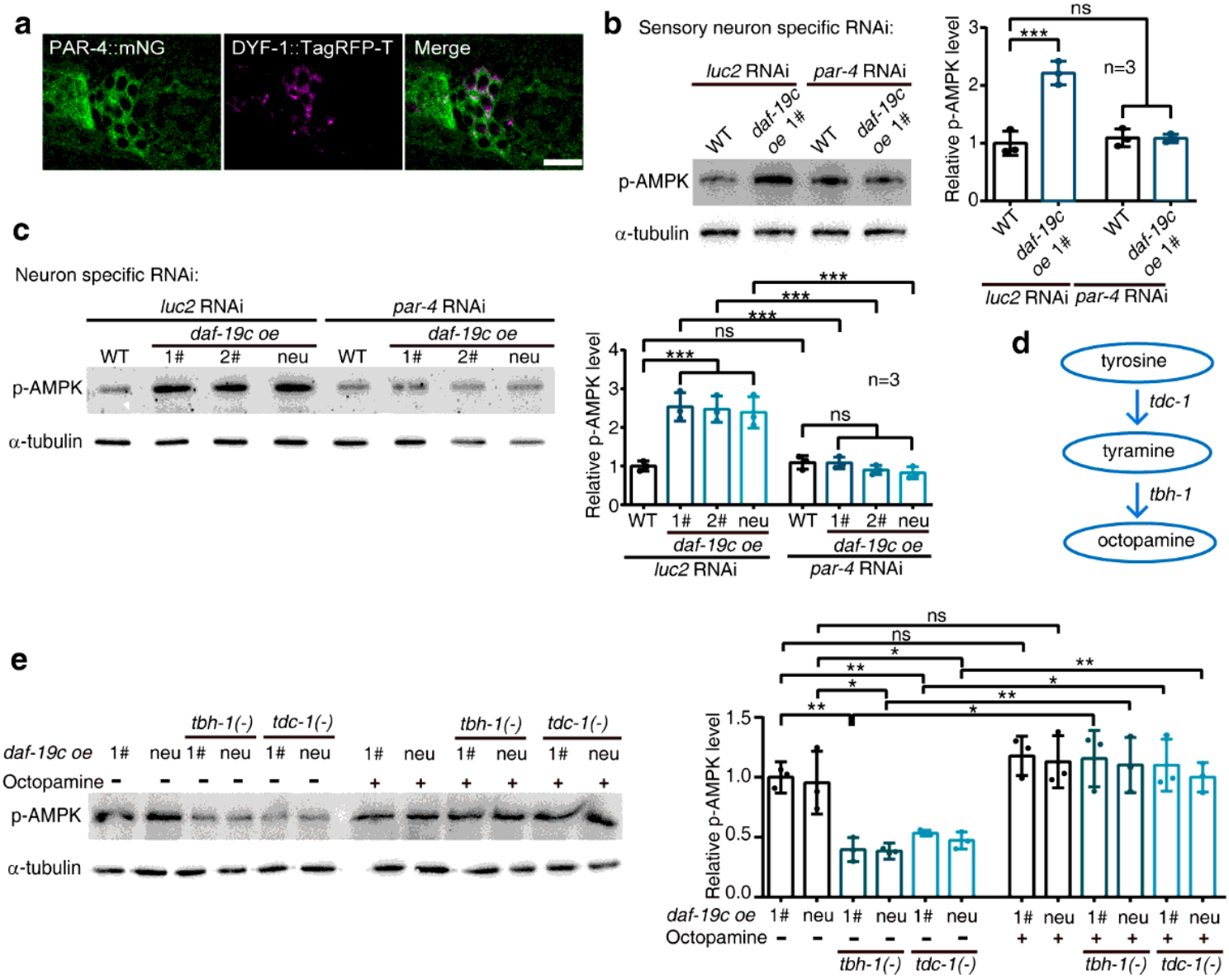


## Figure 5

The enhanced sensory perception upregulates AMPK activity through par-4 and octopamine. a. PAR-4 (green) is expressed in neurons, including sensory neurons. The endogenous par-4 gene was tagged with mNeonGreen (mNG) using CRISPR/Cas9 technology. DYF-1::TagRFP-T (magenta) marks sensory neurons. Scale bar: 10 μm. b. Inhibiting par-4 specifically in sensory neurons blocks the increased p-AMPK in the worms overexpressing daf-19c at day 1 of adulthood. c. The neuron specific RNAi against par-4 blocks the upregulation of p-AMPK in worms overexpressing daf-19c. d. tdc-1 and tbh-1 are two genes encoding critical enzymes in octopamine synthesis. e. The levels of p-AMPK in the indicated worms. Worms were collected at day 1 of adulthood post 30 min of 4 mM octopamine or mock treatment. α-tubulin serves as loading controls in western blot assays. Error bars: SD. Unpaired t-test in (e), One-way ANOVA in the rest, * p<0.05, ** p<0.01, *** p<0.001, ns: non-significant.

**Fig. 6 Zhang et.al**

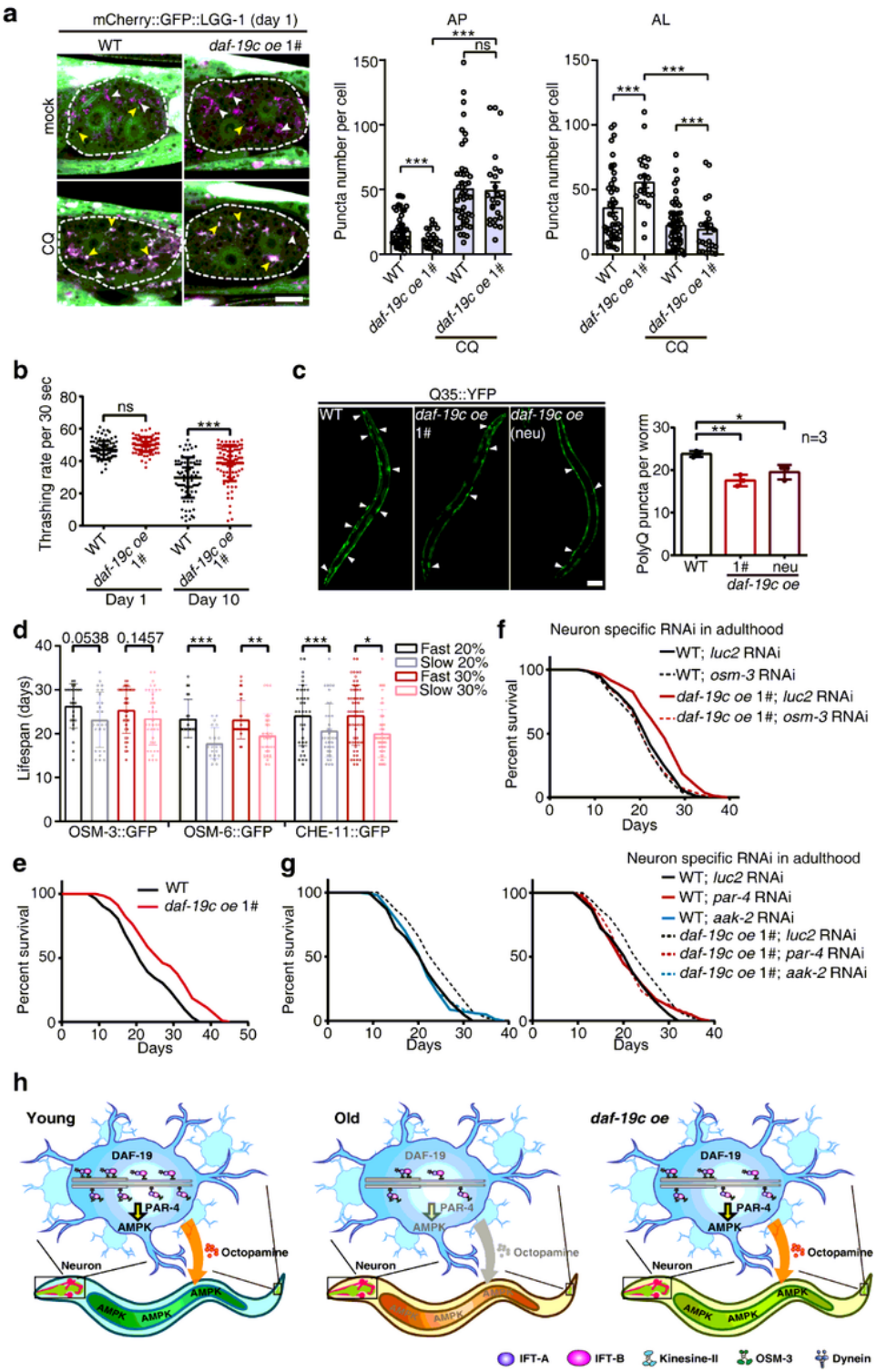


## Figure 6

Improving sensory perception promotes the health and survival of worms. a. Autophagosomes (APs, yellow arrowheads) and autolysosomes (ALs, white arrowheads) in the intestine cells (dashed lines) of indicated strains at day 1 of adulthood post 1 h of 5 mM chloroquine (CQ) or mock treatment. n = 3 independent experiments with at least 20 worms. Scale bar: 10 μm. b. The thrashing rates (a metric for motility) of the indicated worms at day 1 and 10 of adulthood. c. Overexpressing daf-19c reduces polyQ-

YFP aggregates (arrowheads) in body wall muscle. Scale Bar: 100 μm. d. Worms with faster IFT at day 10 of adulthood live longer. Worms were measured for the velocities of the indicated IFT components and subjected to lifespan analysis. e. Overexpressing daf-19c extends lifespan. f-g. Survival curves of WT worms and the worms overexpressing daf-19c undergoing indicated RNAi treatments. Note that disrupting cilia (f) or blocking AMPK signalling (g) abolishes the daf-19c-induced longevity. h. A graphic summary. In aged worms, the impaired IFT in sensory cilia blunts sensory perception and dysregulates AMPK signalling first in sensory neurons through par-4/LKB1 and in turn in other tissues such as the intestine. Overexpressing daf-19c enhances IFT, improves sensory perception and in turn activates AMPK and autophagy. See discussion for details. Error bars: SD. Poisson regression in (a), one-way ANOVA in (b, c), unpaired t-test in (d), * $p<0.05$, ** $p<0.01$, *** $p<0.001$, ns: non-significant. See Supplementary Table 3 for the lifespan statistics in (e-g).

## Supplementary Files

This is a list of supplementary files associated with this preprint. Click to download.

- Zhangetal.SupplementaryTable1AllelesandStrains.xlsx
- Zhangetal.SupplementaryTable2Oligos.xlsx
- Zhangetal.SupplementaryTable3Statistics.xlsx